

Approximation of solutions to the Helmholtz equation from scattered data *

Gilles Chardon, Albert Cohen and Laurent Daudet

December 11, 2013

Abstract

We consider the problem of reconstructing general solutions to the Helmholtz equation $\Delta u + \lambda^2 u = 0$, for some fixed $\lambda > 0$, on some domain $\Omega \subset \mathbb{R}^2$ from the data of these functions at scattered points $x_1, \dots, x_n \in \Omega$. This problem typically arises when sampling acoustic fields with n microphones for the purpose of reconstructing this field over a region of interest Ω that is contained in a larger domain D over which the acoustic field is generated. In many applied settings, the boundary conditions satisfied by the acoustic field on ∂D are unknown as well as the exact shape of D . Our reconstruction method is based on the approximation of a general solution u by linear combinations of Fourier-Bessel functions or plane waves $e_{\mathbf{k}}(x) := e^{i\mathbf{k} \cdot x}$ with $|\mathbf{k}| = \lambda$. We study two different ways of discretizing the infinite dimensional space V_λ of solutions to the Helmholtz equation, leading to two different types of finite dimensional approximation subspaces, and we analyze the convergence of the least squares estimates to u in these subspaces based on the samples $(u(x_i))_{i=1, \dots, n}$. Our analysis describes the amount of regularization that is needed to guarantee the convergence of the least squares estimate towards u , in terms of a condition that depends on the dimension of the approximation subspace and the sample size n . This condition also involves the distribution of the samples and reveals the advantage of using non-uniform distributions that have more points near or on the boundary of Ω . Numerical illustrations show that our approach compares favorably with reconstruction methods using other basis functions, and other types of regularization.

1 Introduction

A common problem in acoustics is to obtain a precise approximation of the soundfield over a spatial domain Ω of interest, using the smallest possible number of pointwise measurements, e.g. as provided by microphones. For instance, one may wish to measure the complex radiation pattern of an extended source (source identification problem), to localize a number of point sources within a spatial domain (source localization problem), or to optimize the output of a sound reproduction system over a large control area, to name only a few applications. In practice, the main difficulty that one is usually faced with is how to handle reverberation : the reverberant field might well be of a magnitude comparable to the direct sound, and it depends in a non-trivial way on both the geometry of the domain D where the acoustic field is defined and the type of boundary conditions on ∂D (with Dirichlet or Neumann as ideal cases, but more likely in engineering problems with a frequency-dependent mixed behaviour).

The goal of this paper is to study the accuracy that can be achieved when approximating the acoustic field over the domain $\Omega \subset D$, based on a set of point measurements, *without precise knowledge on the geometry*

*This research is supported by the ANR project Défi08 ECHANGE.

of D and boundary conditions on ∂D . A general setting is the following: the soundfield $p(x, t)$ is measured at microphones located at positions $x_1, \dots, x_n \in \Omega$, and over a (discretized) time interval $[0, T]$. After application of the (discrete) Fourier transform \mathcal{F} in the time variable, and considering a given frequency ω , the function

$$u(x) := \mathcal{F}p(x, \omega)$$

is a solution on D to the Helmholtz equation

$$\Delta u + \lambda^2 u = 0, \quad (1.1)$$

where $\lambda = \omega/c$, with c denoting the wave velocity, and where the boundary conditions are unknown to us.

Depending on the applications, the geometry of the domain Ω may either be 2-D (membranes) or 3-D (rooms). Here, we restrict our attention to the 2-D setting, although certain features of our approach are readily extendable to the 3-D setting. Our problem therefore amounts to reconstructing, on some domain $\Omega \subset \mathbb{R}^2$, a general solution to the Helmholtz equation (1.1) from its sampling at points $x_1, \dots, x_n \in \Omega$. These samples may be measured exactly or up to some additive noise. We denote by

$$y_l = u(x_l) + \eta_l, \quad l = 1, \dots, n, \quad (1.2)$$

these samples, where η_l represent the additive noise.

Reconstruction from scattered points is a widely studied topic, and a variety of methods have been proposed and analyzed. Many existing methods can be viewed as reconstructing some form of approximation to the unknown function u by simpler functions such as splines, partial Fourier sums or radial basis functions. The success of these methods therefore relies in good part on the quality of the approximation of u by such simpler functions, which is typically governed by the smoothness of u .

In our present setting, the fact that u obeys the Helmholtz equation, may be used in addition to its smoothness in order to guarantee the accuracy of certain approximation schemes, which are well adapted to such solutions. We introduce the Fourier-Bessel functions

$$b_{\lambda,j}(x) := e^{ij\theta} J_j(\lambda r) \quad (1.3)$$

where (r, θ) are the polar coordinates of x and J_j is the j -th Bessel function of the first kind. $b_{\lambda,j}$ is solution to the Helmholtz equation (1.1) over \mathbb{R}^2 if and only if its parameter λ is the same as in (1.1). Denoting V_λ the set of the solutions of (1.1), it is known [4] that

$$V_\lambda = \overline{\text{span}\{b_{\lambda,j}\}}^{L^2(\Omega)}, \quad (1.4)$$

and that the solutions of (1.1) can be approximated by elements of the subspaces $V_m^b = \text{span}\{b_{\lambda,j}, -m \leq j \leq m\}$ as m grows.

An alternative approximation scheme uses plane waves defined by

$$e_{\mathbf{k}}(x) := e^{i\mathbf{k} \cdot x} \quad (1.5)$$

which are solutions of (1.1) if and only if $|\mathbf{k}| = \lambda$. The spaces V_m^e , spanned by the particular plane waves

$$e_j := e_{\mathbf{k}_j}, \quad \mathbf{k}_j := \lambda \left(\cos\left(\frac{2j\pi}{2m+1}\right), \sin\left(\frac{2j\pi}{2m+1}\right) \right), \quad j = -m, \dots, m, \quad (1.6)$$

can also be used to approximate solutions of (1.1) as m grows [4].

The most widely used approach to approximate u in a finite dimensional space V_m , from its data at points x_1, \dots, x_n , is the least squares method, namely with $m \leq n$ solving the minimization problem

$$\pi = \operatorname{argmin}_{v \in V_m} \frac{1}{n} \sum_{i=1}^n |y_i - v(x_i)|^2. \quad (1.7)$$

The effectiveness of the least squares approximation is governed by a certain trade-off in the choice of the dimension m of the approximation:

- A small value of m leads to a highly regularized reconstruction of u , which is usually robust but has poor accuracy.
- A large value of m may lead to unstable and therefore inaccurate reconstructions although the space V_m contains finer approximants to u .

Let us observe that regularization is relevant even in a noiseless context where the function is measured exactly: for example choosing $m = n$ corresponds to searching for an exact interpolation of the data which may be very unstable and inaccurate, similar to the Runge phenomenon in polynomial approximation.

In this paper, we discuss the amount of regularization which is needed when applying the least squares method using the finite dimensional subspaces V_m^b and V_m^e extracted from V_λ . With such discretizations, the distribution of the sampling points x_1, \dots, x_n has an influence on the above described trade-off. Our main theoretical result, established in the case of a disc, shows that higher values of m , leading therefore to better accuracy, can be used if the x_i are not uniformly distributed on Ω in the sense that a fixed fraction of these points are located on the boundary $\partial\Omega$. This result is confirmed by numerical experiments.

The rest of this paper is organized as follow: we give a brief account in §2 on approximation of solutions to (1.1) by Fourier-Bessel functions and plane waves which relies on Vekua's theory, and in §3 on general results on the stability and accuracy of least-squares approximations recently established in [2]. We then study in §4 the spaces V_m^e and V_m^b in more detail, in the particular case where Ω is a disc, and use the above mentioned results to compare least-squares approximations on these spaces based on different sampling strategies. In §5, we present numerical tests that illustrate the validity of this comparison. We also show that our approach compares favorably with reconstructions based on other approximation schemes such as partial Fourier sums (that do not exploit the fact that u is a solution to (1.1)) and to other form of regularizations such as Orthogonal Matching Pursuit.

2 Approximation by Fourier-Bessel functions and plane waves

Results on the approximation of solutions to (1.1) by Fourier-Bessel functions and plane waves given in [4] are based on the theory developed in the 1950's by Vekua [6]. This theory generalizes approximation results for holomorphic functions, viewed as solutions of $\Delta u = 0$, to solutions of more general elliptic partial differential equations, by means of appropriate operators that link the two types of solutions.

In the case of the Helmholtz equation on a domain Ω , that is star-shaped with respect to a point which is fixed as the origin 0, these operators (in their version mapping harmonic functions to solutions of (1.1)) have the explicit expression

$$\mathcal{V}_1 \phi(x) = \phi(x) - \frac{\lambda|x|}{2} \int_0^1 \frac{1}{\sqrt{1-t}} J_1(\lambda|x|\sqrt{1-t}) dt, \quad (2.1)$$

and

$$\mathcal{V}_2\phi(x) = \phi(x) + \frac{\lambda|x|}{2} \int_0^1 \frac{1}{\sqrt{t(1-t)}} I_1(\lambda|x|\sqrt{1-t}) dt, \quad (2.2)$$

where $|x|$ stands for the euclidean norm of x , J_1 is the Bessel function of the first kind of order 1 and I_1 the modified Bessel function of the first kind of order 1, see [3] for more details. These operators have important properties:

- Their are linear.
- \mathcal{V}_1 maps harmonic functions to solutions of the Helmholtz equation, and \mathcal{V}_2 does the converse.
- They are continuous in the Sobolev H^k norms for all $k \geq 0$.
- They are inverse to each other on these spaces.

As a consequence, any approximation method for harmonic functions can be translated as an approximation method for solutions of the Helmholtz equation. In particular, approximation of harmonic functions by harmonic polynomials of degree m translates as approximation of solution of the Helmholtz equation by the so-called generalized harmonic polynomials m which are their image by V_1 . The generalized harmonic polynomials of degree m can be expressed as linear combinations of the Fourier-Bessel functions (1.3), leading therefore to results for the approximation of solutions to (1.1) by elements of V_m^b in Sobolev norms. More precisely, the following result can be obtained when the domain Ω is convex, see theorem 3.2 of [4]

$$\min_{v \in V_m^b} \|u - v\|_{H^k} \leq C \left(\frac{\log m}{m} \right)^{p-k} \|u\|_{H^p}, \quad (2.3)$$

where the constant C depends on p , k , λ and the geometry of Ω . This results still holds for more general, star-shaped convex domains, with a slower convergence.

Planes waves and Bessel functions are related by the Jacobi-Anger identity

$$e_{\mathbf{k}_\phi} = \sum_{m \in \mathbb{Z}} i^m J_m(\lambda r) e^{im(\theta - \phi)}. \quad (2.4)$$

where $\mathbf{k}_\phi := \lambda(\cos(\phi), \sin(\phi))$, and its converse, the Bessel integral

$$J_n(\lambda r) e^{in\theta} = \frac{1}{2\pi i^n} \int_{-\pi}^{\pi} e_{\mathbf{k}_\phi} e^{in\phi} d\phi, \quad (2.5)$$

Approximating the integral in (2.5) by a discrete sum, with uniformly sampling of the wave vectors \mathbf{k}_ϕ on the circle of diameter λ , leads to approximations of solutions to (1.1) by linear combinations of the $2m+1$ planes waves $e_{\mathbf{k}_j}$, that is, by elements of V_m^e . It is also known (see theorem 5.2 of [4]) that such approximations have the same convergence properties, e.g., for a convex domain,

$$\min_{v \in V_m^e} \|u - v\|_{H^k} \leq C \left(\frac{\log m}{m} \right)^{p-k} \|u\|_{H^p}. \quad (2.6)$$

3 Least-square approximations

The results of the previous section quantify how a general solution u of the Helmholtz equation can be approximated by functions from spaces V_m^e or V_m^b . We are now interested in understanding the quality of approximations from these spaces built by the least squares methods based on scattered data $(x_l, y_l)_{l=1, \dots, n}$. In particular, we want to understand the trade-off between the dimension m and the number of samples n . Ideally we would like to choose m large in order to benefit of the approximation properties (2.3) and (2.6), however not too large so that stability of the least-square method is ensured. We are also interested in understanding how the spatial distribution of the sample x_l influences this trade-off.

This problem was recently studied in [2], in a general setting where the x_l are independently drawn according to a given probability measure ν defined on Ω . This measure therefore reflects the spatial distribution of the samples. For example, the uniform measure

$$d\nu := |\Omega|^{-1} dx, \quad (3.1)$$

tends to generate uniformly spaced samples. In order to present the general result of [2], we assume that $(V_m)_{m \geq 1}$ is an arbitrary sequence of finite dimensional spaces of functions defined on Ω with $\dim(V_m) = m$.

We introduce the L^2 norm with respect to the measure ν

$$\|v\| := \left(\int_{\Omega} |v|^2 d\nu \right)^{1/2}, \quad (3.2)$$

and we define the best approximation error for a function u in this norm as

$$\sigma_m(u) := \min_{v \in V_m} \|u - v\| \quad (3.3)$$

Note that, in the noiseless case, the least squares method amounts to computing the best approximation of u onto V_m with respect to the norm

$$\|v\|_n := \left(\frac{1}{n} \sum |v(x_l)|^2 \right)^{1/2}. \quad (3.4)$$

This norm can be viewed as an approximation of the norm $\|v\|$ based on the draw, and it is therefore natural to compare the error $\|u - \pi\|$ where π is computed by (1.7) with $\sigma_m(u)$. We give below a criterion that describes under which condition on m these two quantities are of comparable size.

Here, we assume that (L_1, \dots, L_m) is a basis of V_m which is orthonormal in $L^2(\Omega, \nu)$. We define the quantity

$$K(m) = K(V_m, \nu) := \max_{x \in \Omega} \sum_{j=1}^m |L_j(x)|^2, \quad (3.5)$$

which depends both on V_m and on the chosen measure ν , but not on the choice of the orthonormal basis since it is invariant by rotation.

We also assume that an a-priori bound $\|u\|_{L^\infty} \leq M$ is known on the function u . We can therefore only improve the least squares estimate by defining

$$\tilde{u} := T_M(\pi), \quad (3.6)$$

where $T_M(t) := \text{sign}(t) \max\{|t|, M\}$ and π is given by (1.7). The following result was established in [2], in the case of noiseless data, i.e. $\eta_l = 0$ in (1.2).

Theorem 3.1 *Let $r > 0$ be arbitrary but fixed and let $\kappa := \frac{1-\log 2}{2+2r}$. If m is such that*

$$K(m) \leq \kappa \frac{n}{\log n}, \quad (3.7)$$

then, one has

$$E(\|u - \tilde{u}\|^2) \leq (1 + \varepsilon(n))\sigma_m(u)^2 + 8M^2n^{-r}, \quad (3.8)$$

where $\varepsilon(n) := \frac{4\kappa}{\log n} \rightarrow 0$ as $n \rightarrow +\infty$.

It is also established in [2] that the condition (3.7) ensures the numerical stability of the least-square method, with probability larger than $1 - 2n^{-r}$. These results suggest to set the regularization level by picking the largest value of $m^* = m^*(n)$ such that (3.7) holds. The dependance of $m^*(n)$ with n is obviously related to that of $K(m)$ with m . In particular, slower growth of $K(m)$ with m implies faster growth of $m^*(n)$ and therefore faster convergence of the least squares approximation. Notice that we always have

$$K(m) \geq \int_{\Omega} \sum_{j=1}^m |L_j|^2 d\nu = m. \quad (3.9)$$

In the next section, we evaluate $K(V_m^e, \nu)$ and $K(V_b^e, \nu)$ in the case where Ω is a disk, for various choices of the measure ν .

4 Fourier-Bessel functions and plane waves on the disc

As mentioned in the previous section, the quantity $K(m)$ depends both on the space V_m and the measure ν that reflects the sampling strategy. Here we study the case where V_m is either one of the spaces of plane waves V_m^e or of Fourier-Bessel functions V_m^b defined in the introduction. Note that the dimension of these spaces is not m but $2m + 1$, but for notational simplicity we maintain the shorthand $K(m)$ for $K(V_m^e, \nu)$ and $K(V_b^e, \nu)$.

We consider two sampling strategies. The first one uses the uniform probability distribution

$$\nu_0 := \frac{dx}{|\Omega|}, \quad (4.1)$$

and the second one combines uniform sampling on the domain and on its boundary, with proportion $0 < \alpha \leq 1$, according to the probability distribution

$$\nu_{\alpha} := (1 - \alpha) \frac{dx}{|\Omega|} + \alpha \frac{d\sigma}{|\partial\Omega|}. \quad (4.2)$$

In order to obtain explicit results, we focus on the simple case where Ω is a disk. Without loss of generality, we fix

$$\Omega := \{x \in \mathbb{R}^2 : |x| \leq 1\}. \quad (4.3)$$

4.1 Fourier-Bessel approximation

Fourier-Bessel functions are orthogonal on the disk with respect to any rotation-invariant measure, because of their angular dependence in $e^{in\theta}$. This allows a simple computation of the quantity $K(m)$ for the space V_m^b , leading to the following result.

Theorem 4.1 For the space V_m^b and the measure ν_α on the unit disk Ω , one has for sufficiently large m

$$K(m) \geq c_0 + c_1 m^2, \quad (4.4)$$

when $\alpha = 0$ (that is, for the uniform measure), for any $c_1 < 1/4$, and where c_0 depends on c_1 and λ , and

$$K(m) \leq C + \frac{2m}{\alpha}, \quad (4.5)$$

when $\alpha > 0$, where C depends on λ and α .

Proof: Since the Fourier-Bessel functions are orthogonal in $L^2(\Omega, \nu_\alpha)$, we have

$$K(m) = \left\| \sum_{j=-m}^m \frac{|b_j|^2}{\|b_j\|^2} \right\|_{L^\infty(\Omega)}. \quad (4.6)$$

In the case of the uniform measure, we bound $K(m)$ from below. We first write

$$K(m) \geq \left\| \sum_{j=-m}^m \frac{|b_j|^2}{\|b_j\|^2} \right\|_{L^\infty(\partial\Omega)}. \quad (4.7)$$

We next bound $\|b_j\|^2$, for $j > \lceil \lambda \rceil$ (the case $j < -\lceil \lambda \rceil$ is identical, as $|b_j| = |b_{-j}|$), according to

$$\begin{aligned} \|b_j\|^2 &= \frac{1}{\pi} \int_{\Omega} J_j(\lambda|x|)^2 dx \\ &= 2 \int_0^1 r J_j(\lambda r)^2 dr \\ &= \frac{4}{\lambda^2} \sum_{p=0}^{\infty} (j+1+2p) J_{j+1+2p}^2(\lambda) \\ &\leq \frac{4}{\lambda^2} \sum_{p=0}^{\infty} (j+1+2p) (\lambda/j)^{2+4p} J_j^2(\lambda) \\ &= 4 \frac{j+1}{j^2} \left(\frac{1}{1 - (\lambda/j)^4} + \frac{2}{j+1} \frac{(\lambda/j)^4}{(1 - (\lambda/j)^4)^2} \right) J_j^2(\lambda) \end{aligned}$$

where the third equality is identity (11.3.32) of [1] for the third equality, and the first inequality comes from (A.6) of [5]. As $|b_j(1, \theta)| = |J_j(\lambda)|$, we have

$$\frac{|b_j(1, \theta)^2|}{\|b_j\|^2} \geq \frac{j^2}{4(j+1)} \left(\frac{1}{1 - (\lambda/j)^4} + \frac{2}{j+1} \frac{(\lambda/j)^4}{(1 - (\lambda/j)^4)^2} \right)^{-1} \sim \frac{j}{4} \quad (4.8)$$

For any $c < 1$, there exists a j_0 such that when $j > j_0$,

$$\frac{|b_j(1, \theta)^2|}{\|b_j\|^2} \geq c \frac{j}{4} \quad (4.9)$$

and

$$K(m) \geq \sum_{j=-j_0}^{j_0} \frac{|J_j(\lambda)|^2}{\|b_j\|^2} + 2c \sum_{j_0 < j \leq m} \frac{j}{4} \quad (4.10)$$

$$\geq \sum_{j=-j_0}^{j_0} \frac{|J_j(\lambda)|^2}{\|b_j\|^2} - c \frac{j_0(j_0+1)}{4} + \frac{c}{4} m(m+1) \quad (4.11)$$

which proves the bound (4.4) when $m > j_0$.

In the case of mixed sampling, we bound $K(m)$ from above by

$$K(m) \leq \sum_{j=-m}^m \frac{\|b_j\|_{L^\infty(\Omega)}^2}{\|b_j\|^2}$$

When $j > \lambda$, the function $r \mapsto J_l(\lambda r)$ is monotone increasing on $[0, 1]$, so that $\|b_j\|_{L^\infty(\Omega)} = J_j(\lambda)$. Thus,

$$\begin{aligned} \frac{\|b_j\|_{L^\infty(\Omega)}}{\|b_n\|^2} &= \frac{J_j(\lambda)^2}{\frac{1-\alpha}{\pi} \int_D J_j(\lambda|x|)^2 dx + \frac{\alpha}{2\pi} \int_0^{2\pi} J_j(\lambda)^2 d\theta} \\ &< \frac{1}{\alpha} \end{aligned}$$

We then have

$$K(m) \leq \frac{2(m - \lfloor \lambda \rfloor)}{\alpha} + \sum_{j=-\lfloor \lambda \rfloor}^{\lfloor \lambda \rfloor} \frac{\|b_j(x)\|_{L^\infty(\Omega)}^2}{\|b_j\|^2}$$

which proves (4.5).

4.2 Plane wave approximation

Similar results can be obtained for the plane wave approximation:

Theorem 4.2 *For the space V_m^e and the measure ν_α on the unit disk Ω , one has for sufficiently large m*

$$K(m) \geq c_0 + c_1 m^2, \quad (4.12)$$

when $\alpha = 0$ (that is, for the uniform measure), for any $c_1 < 1/4$, where c_0 depends on c_1 and λ , and

$$K(m) \leq C_1 + C_2 \frac{2m}{\alpha}, \quad (4.13)$$

when $\alpha > 0$, for any $C_2 > 1$, where C_1 depends on C_2 , λ and α .

Proof: Since plane waves are not orthogonal in $L^2(\Omega, \nu)$, the first step is the computation of an orthogonal basis of the space spanned by these plane waves. Let us consider $2m + 1$ plane waves, with wave vectors uniformly distributed on the circle of radius λ . For the measures considered here, the Gram matrix of this family is a circulant matrix, which is diagonalized in the Fourier basis. An orthogonal family spanning the same space is therefore given by functions that are linear combinations of plane waves with the coefficients of the discrete Fourier transform:

$$b_j^m := \frac{1}{(2m+1)} \sum_{j=-m}^m e^{2\pi i j/(2m+1)} e_{\mathbf{k}_j} \quad (4.14)$$

This formula may be thought as a quadrature for the Bessel integral (2.5): the b_j^m are thus approximations of the Fourier-Bessel functions b_j . In order to bound the quantity $K(m) = K(V_m^e, \nu)$, we compare it to the quantity $K(V_m^b, \nu)$ which behaviour is described by Theorem 4.1. Using (8) and (9) from [5] we have

$$b_j^m = \sum_{p \in \mathbb{Z}} i^{p(2m+1)} b_{j+p(2m+1)}, \quad (4.15)$$

and

$$\left| \frac{b_j^m}{b_j} - 1 \right| \leq \sum_{p \in \mathbb{Z} - \{0\}} \frac{|b_{j+p(2m+1)}|}{|b_j|}. \quad (4.16)$$

With $m \geq j \geq \lambda$, we thus have for all $0 \leq r \leq 1$ and $0 \leq \theta \leq 2\pi$,

$$\begin{aligned} \left| \frac{b_j^m(r, \theta)}{b_j(r, \theta)} - 1 \right| &\leq \frac{1}{|b_j(r, \theta)|} \left(\sum_{p \geq 0} |b_{j+(p+1)(2m+1)}(r, \theta)| + \sum_{p \geq 0} |b_{j+(p+1)(2m+1)-2j}(r, \theta)| \right) \\ &\leq \sum_{p \in \mathbb{N}} \left(1 + \left(\frac{\lambda}{j} \right)^{-2j} \right) \left(\frac{\lambda}{j} \right)^{(p+1)(2m+1)} \\ &= \frac{\left(\frac{\lambda}{j} \right)^{2m+1} + \left(\frac{\lambda}{j} \right)^{2m+1-2j}}{1 - \left(\frac{\lambda}{j} \right)^{2m+1}} \\ &\leq \frac{2 \frac{\lambda}{j}}{1 - \frac{\lambda}{j}} \end{aligned}$$

where we have used equation (A.6) of [5] to obtain the second inequality.

Using the orthogonality of the b_j , we have

$$\|b_j^m\|^2 = \sum_{p \in \mathbb{Z}} \|b_{j+p(2m+1)}\|^2, \quad (4.17)$$

and

$$\left| \frac{\|b_j^m\|^2}{\|b_j\|^2} - 1 \right| = \sum_{p \in \mathbb{Z} - \{0\}} \frac{\|b_{j+p(2m+1)}\|^2}{\|b_j\|^2}. \quad (4.18)$$

When $j \geq \lambda$ and $l \geq 0$ we bound $\|b_{j+l}\|^2$ according to

$$\begin{aligned} \|b_{j+l}\|^2 &= 2\pi \int_0^1 r J_{j+l}(\lambda r)^2 dr \\ &\leq 2\pi \int_0^1 r \left(\frac{\lambda r}{j} \right)^{2l} J_j(\lambda r)^2 dr \\ &\leq \left(\frac{\lambda}{j} \right)^{2l} 2\pi \int_0^1 J_j(\lambda r)^2 dr \\ &= \left(\frac{\lambda}{j} \right)^{2l} \|b_j\|^2 \end{aligned}$$

where we again have used equation (A.6) of [5] to obtain the first inequality. We thus have

$$\begin{aligned} \left| \frac{\|b_j^m\|^2}{\|b_j\|^2} - 1 \right| &= \sum_{p \in \mathbb{Z} - \{0\}} \frac{\|b_{j+p(2m+1)}\|^2}{\|b_j\|^2} \\ &= \frac{1}{\|b_j\|^2} \left(\sum_{p \geq 0} \|b_{j+(p+1)(2m+1)}\|^2 + \sum_{p \geq 0} \|b_{j+(p+1)(2m+1)-2j}\|^2 \right) \end{aligned}$$

$$\begin{aligned}
&\leq \left(\sum_{p \geq 0} \left(\frac{\lambda}{j} \right)^{2(p+1)(2m+1)} + \sum_{p \geq 0} \left(\frac{\lambda}{j} \right)^{2((p+1)(2m+1)-2j)} \right) \\
&= \frac{\left(\frac{\lambda}{j} \right)^{2(2m+1)} + \left(\frac{\lambda}{j} \right)^{2(2m+1-2j)}}{1 - \left(\frac{\lambda}{j} \right)^{2(2m+1)}} \\
&\leq \frac{2 \left(\frac{\lambda}{j} \right)^2}{1 - \left(\frac{\lambda}{j} \right)^2}
\end{aligned}$$

We now consider the case $\alpha = 0$. Using the above comparison results between b_j and b_j^m , we can find, for any $c < 1$ a positive integer j_c such that for $m \geq j \geq j_c$,

$$\frac{|b_j^m(1, \theta)|^2}{\|b_j^m\|^2} \geq c \frac{J_j(\lambda)^2}{\|b_j\|^2}. \quad (4.19)$$

We may thus write

$$\begin{aligned}
K(V_m^e, \nu) &= \left\| \sum_{j=-m}^m \frac{|b_j^m|^2}{\|b_j^m\|^2} \right\|_{L^\infty(\Omega)} \\
&\geq \sum_{j=-m}^m \frac{|b_j^m(1, 0)|^2}{\|b_j^m\|^2} \\
&\geq \sum_{j < j_c} \frac{|b_j^m(1, 0)|^2}{\|b_j^m\|^2} + 2c \sum_{j=j_c}^m \frac{J_j(\lambda)^2}{\|b_j\|^2}, \\
&\geq 2c \sum_{j=j_c}^m \frac{J_j(\lambda)^2}{\|b_j\|^2}.
\end{aligned}$$

The last sum can be bounded from below in a similar way as in the proof of Theorem 4.1, proving (4.12).

We next consider the case $\alpha > 0$. We then write

$$K(m) \leq \sum_{j=-m}^m \frac{\|b_j^m\|_{L^\infty(\Omega)}^2}{\|b_j^m\|^2}. \quad (4.20)$$

For any $C > 1$, there is a $j_C > \lambda$ such that when $j > j_C$, we have $\frac{1}{C}|b_j(r, \theta)| \leq |b_j^m(r, \theta)| \leq C|b_j(r, \theta)|$, so that $\|b_j^m\|_{L^\infty(\Omega)} < C\|b_j\|_{L^\infty(\Omega)} = CJ_j(\lambda)$, and $|b_j^m(1, \theta)| \geq |J_j(\lambda)|/C$. We then have, for $m \geq j \geq j_C$,

$$\begin{aligned}
\frac{\|b_j^m\|_{L^\infty(\Omega)}^2}{\|b_j^m\|^2} &= \frac{\|b_j^m\|_{L^\infty(\Omega)}^2}{\frac{1-\alpha}{\pi} \int_D |b_j^m|^2 dx + \frac{\alpha}{2\pi} \int_0^{2\pi} |b_j^m|^2 d\theta} \\
&\leq \frac{1}{\alpha} \frac{C^2 J_j(\lambda)^2}{J_j(\lambda)^2 / C^2} \\
&\leq \frac{C_2}{\alpha}
\end{aligned}$$

and

$$\begin{aligned} K(m) &\leq \frac{2C_2(m - \lfloor \lambda \rfloor)}{\alpha} + \sum_{|j| < j_0} \frac{\|b_j^m\|_{L^\infty(\Omega)}^2}{\|b_j^m\|^2} \\ &\leq \frac{2C_2(m - \lfloor \lambda \rfloor)}{\alpha} + \sum_{|j| < j_0} \frac{1}{\|b_j\|^2} \end{aligned}$$

which proves 4.13. We use here the fact that $\|b_j^m\|_{L^\infty(\Omega)} \leq 1$ which is clear from (4.14), and $\|b_j\| \leq \|b_j^m\|$ obtained from (4.15) and the orthogonality of the b_j . \square

5 Numerical tests

Here, we compare three different reconstructions methods on the unit disc:

- (i) The proposed least-squares method, using Fourier-Bessel approximations.
- (ii) The least-squares method, using the space spanned $(2K + 1)^2$ orthogonal Fourier modes on a square enclosing the disc. These modes thus have the form $e^{a\mathbf{k} \cdot \mathbf{x}}$ for some fixed $0 < a \leq \pi$ (here we took $a = \pi$) and $\mathbf{k} \in \{-K, \dots, K\}^2$ and it is assumed that $(2K + 1)^2 < n$. This regularization method is one of the most often used in acoustic applications.
- (iii) The Orthogonal Matching Pursuit algorithm used to select a sparse approximation in a dictionary that consists of the same Fourier modes, now with $(2K + 1)^2 > n$ and $K = 40$.

We fix the wave number to be $\lambda = 12$ and we compare sampling using the measure ν_α for various proportions $0 \leq \alpha \leq 1$.

Results for the proposed method (i) are displayed on Figure 5.1, with $n = 400$ measurements and the different values $\alpha = 0, 0.1, 0.5, 0.9, 1$. We plot the error measured in the norm $L^2(\Omega) = L^2(\Omega, dx)$, averaged over 10 realizations of the sampling, versus the approximation space dimension $2m + 1$. We observe that placing more measurement points on the boundary $\partial\Omega$ is beneficial to the reconstruction: as α approaches 1, the lowest error decreases and is attained for larger values of m , confirming our theoretical results. However, measuring the solutions only on $\partial\Omega$ ($\alpha = 1$) does not yield good reconstructions. In that case, Theorem 3.1 only ensures that the reconstruction is accurate on $\partial\Omega$ and says nothing on the error on the disk itself, since we cannot control the $L^2(\Omega)$ norm by the $L^2(\Omega, \nu_1) = L^2(\partial\Omega)$ norm.

Results with identical parameters for the two other methods (ii) and (iii) are displayed on Figures 5.2 and 5.3. Reconstruction errors for these methods are larger by a few orders of magnitude than the errors of the proposed method (i). Moreover, these two methods do not benefit from sampling on the boundary, as the best results are obtained with the uniform sampling.

Figure 5.4 compares the behavior of these methods “at their best” with varying number of measurements, from 100 to 800. The plotted errors are obtained by selecting the value of m for (i), of K for (ii), and of the number of iterations of OMP for (iii), as well as the proportion α , that minimize the error for the given number n of measurements. Results for (ii) and (iii) are both worse than for the proposed method (i), and are always obtained with $\alpha = 0$. In contrast, the best results of (i) are obtained with α getting closer to 1 as the number n of measurement grows, for instance $\alpha = 0.9$ with $n = 800$ measurements.

In the practice of using the proposed method, the optimal value of m is unknown to us. A simple way of estimating it is by using an independent sample, such as in the generalized cross-validation (GCV) method. As an example, for a given number $2m + 1$ of Fourier-Bessel functions, we estimate a reconstruction using

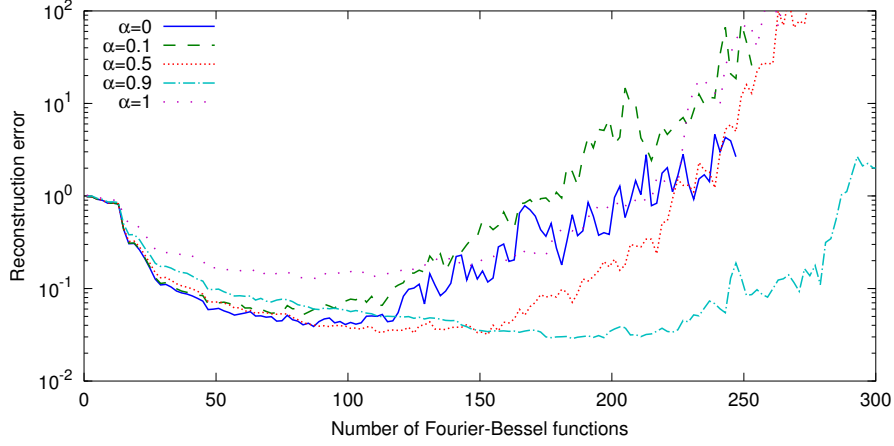


Figure 5.1: Reconstruction error for method (i) vs. number of Fourier-Bessel functions with $n = 400$ measurements

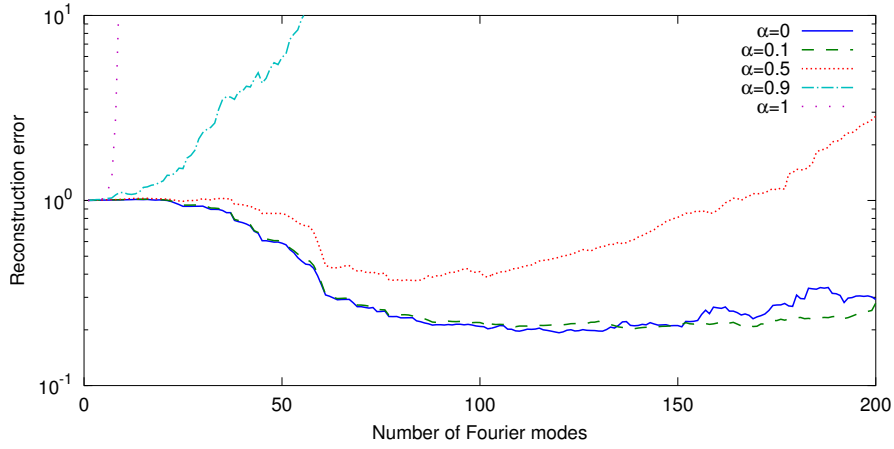


Figure 5.2: Reconstruction error for method (ii) vs. number of Fourier modes with $n = 400$ measurements

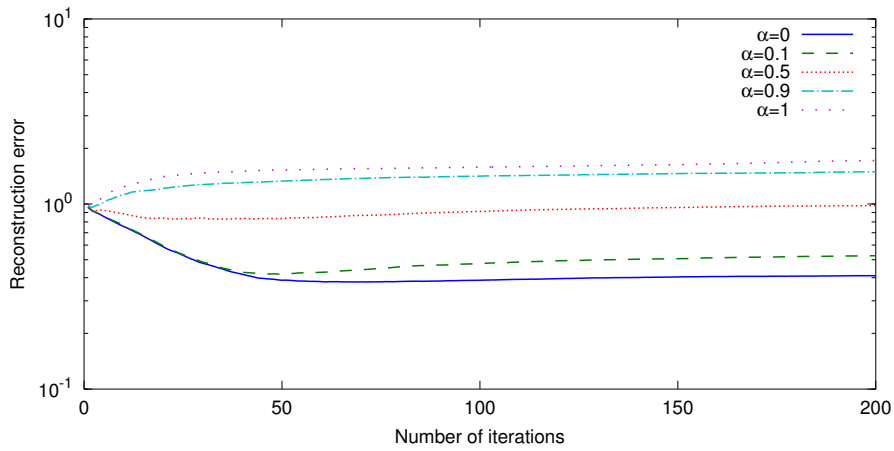


Figure 5.3: Reconstruction error for method (iii) vs. number of OMP iterations, with $n = 400$ measurements

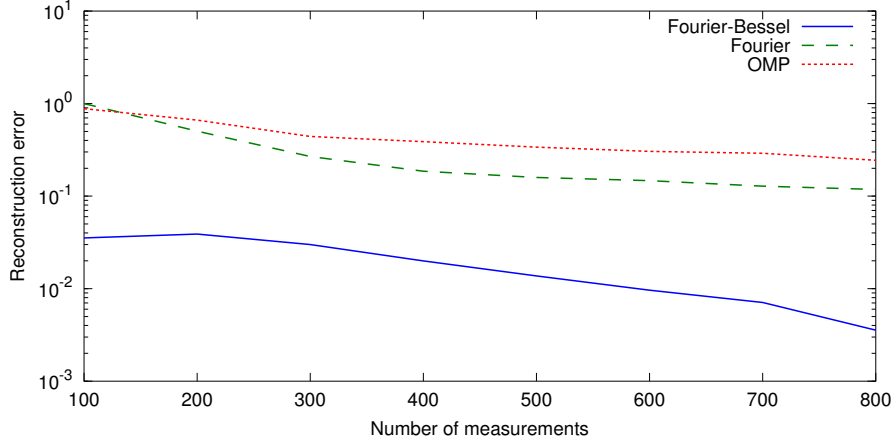


Figure 5.4: Best reconstruction error for method (i) Fourier-Bessel, (ii) Fourier and (iii) OMP

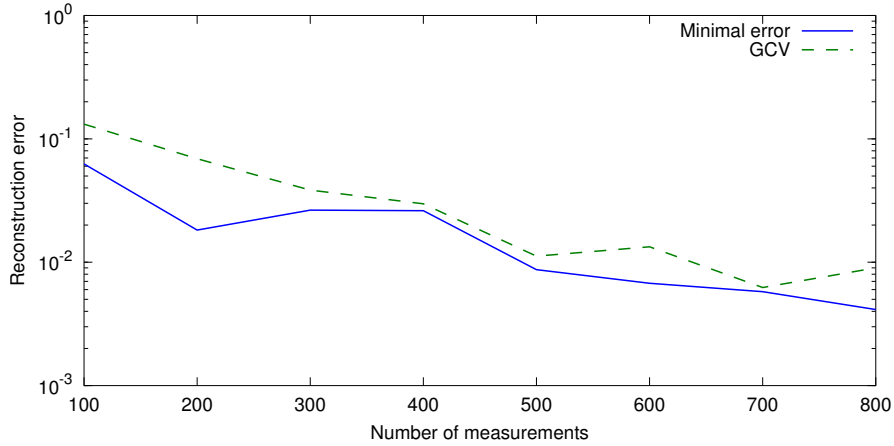


Figure 5.5: Best reconstruction error for method (i), using GCV and optimal value of m .

90% of the samples, and evaluate empirically the mean-square error using the remaining ones. We repeat the estimation 10 times using different choices of estimation and reconstruction points within the same sample, and select the number m that minimizes the mean square error. The function is then reconstructed using all samples. On Figure 5.5, we compare the results obtained by this method with those based on the optimal value of m , as the number of measurement n varies. We observe that the performances are comparable up to a slight loss by a multiplicative constant.

6 Conclusion

In this paper, we compare different ways of sampling solutions of the Helmholtz equation, using a finite number of point measurements. Our main results reveal that good reconstructions can be obtained using Fourier-Bessel or plane waves approximations, and that these reconstructions benefit from a denser sampling on the boundary.

These results were obtained in the particular case of a two-dimensional disc. For a more general star-

shaped domain in \mathbb{R}^2 , the Fourier-Bessel approximation remains valid. The quantity $K(m)$ does not have an explicit expression, yet it can be evaluated numerically after orthogonalization of the Fourier-Bessel family. Our first numerical investigations indicate that denser sampling of the functions on the boundary is also beneficial in this more general setting.

In the 3-D case, solutions to the Helmholtz equation in a star-shaped domain can be approximated in a similar way, using functions that are products of spherical harmonics and spherical Bessel functions. We expect that a refined analysis of these functions, which have certain common properties with the 2-D Fourier-Bessel functions, leads to similar results concerning the convergence of least-squares approximations and the role of a denser sampling on the boundary.

References

- [1] M. Abramowitz and I. A. Stegun, *Handbook of mathematical functions*, Dover, 1964.
- [2] A. Cohen, M. Davenport and D. Leviatan, *On the stability and accuracy of least squares approximation*, submitted to J. FoCM, 2012.
- [3] A. Moiola, R. Hiptmair and I. Perugia, *Vekua theory for the Helmholtz operator*, Z. Angew. Math. Phys. 62-5, 779-807, 2011.
- [4] A. Moiola, R. Hiptmair and I. Perugia, *Plane wave approximation of homogeneous Helmholtz equation*, Z. Angew. Math. Phys. 62-5, 809-837, 2011.
- [5] E. Perrey-Debain, *Plane wave decomposition in the unit disc: Convergence estimates and computational aspects*, J. of Comp. and App. Math., 193-1, 140-156, 2006
- [6] I.N. Vekua *New methods for solving elliptic equations*, North-Holland Pub. Co., 1967

Gilles Chardon

Institut Langevin, UPMC Univ. Paris 06, F-75005, Paris, France

Present address: Acoustics Research Institute, Austrian Academy of Sciences, A-1040, Wien, Austria

gchardon@kfs.oeaw.ac.at

Albert Cohen

UPMC Univ. Paris 06, UMR 7598, Laboratoire Jacques-Louis Lions, F-75005, Paris, France

CNRS, UMR 7598, Laboratoire Jacques-Louis Lions, F-75005, Paris, France

cohen@ann.jussieu.fr

Laurent Daudet

Institut Langevin, Paris Diderot University and Institut Universitaire de France, F-75005, Paris, France

laurent.daudet@espci.fr